



## Growth of organic films on indoor surfaces

Weschler, Charles J.; Nazaroff, W. W.

*Published in:*  
Indoor Air

*Link to article, DOI:*  
[10.1111/ina.12396](https://doi.org/10.1111/ina.12396)

*Publication date:*  
2017

*Document Version*  
Peer reviewed version

[Link back to DTU Orbit](#)

*Citation (APA):*  
Weschler, C. J., & Nazaroff, W. W. (2017). Growth of organic films on indoor surfaces. *Indoor Air*, 27(6), 1101-1112. <https://doi.org/10.1111/ina.12396>

---

### General rights

Copyright and moral rights for the publications made accessible in the public portal are retained by the authors and/or other copyright owners and it is a condition of accessing publications that users recognise and abide by the legal requirements associated with these rights.

- Users may download and print one copy of any publication from the public portal for the purpose of private study or research.
- You may not further distribute the material or use it for any profit-making activity or commercial gain
- You may freely distribute the URL identifying the publication in the public portal

If you believe that this document breaches copyright please contact us providing details, and we will remove access to the work immediately and investigate your claim.

DR. CHARLES J WESCHLER (Orcid ID : 0000-0002-9097-5850)

PROF. WILLIAM W NAZAROFF (Orcid ID : 0000-0001-5645-3357)

Article type : Original Article

## Growth of Organic Films on Indoor Surfaces

Charles J. Weschler<sup>1,2\*</sup> and William W Nazaroff<sup>3</sup>

<sup>1</sup>Environmental and Occupational Health Sciences Institute, University of Medicine and Dentistry of New Jersey and Rutgers University, Piscataway, NJ 08854, USA

<sup>2</sup>International Centre for Indoor Environment and Energy, Technical University of Denmark, DK-2800 Lyngby, Denmark

<sup>3</sup>Department of Civil and Environmental Engineering, University of California, Berkeley, CA 94720-1710, USA

*\*Corresponding email: weschlch@rwjms.rutgers.edu*

### Abstract

We present a model for the growth of organic films on impermeable indoor surfaces. The model couples transport through a gas-side boundary layer adjacent to the surface with equilibrium partitioning of semivolatile organic compounds (SVOCs) between the gas-phase and the surface film. Model predictions indicate that film growth would primarily be

This article has been accepted for publication and undergone full peer review but has not been through the copyediting, typesetting, pagination and proofreading process, which may lead to differences between this version and the Version of Record. Please cite this article as doi: 10.1111/ina.12396

This article is protected by copyright. All rights reserved.

influenced by the gas-phase concentration of SVOCs with octanol-air partitioning ( $K_{oa}$ ) values in the approximate range  $10 \leq \log K_{oa} \leq 13$ . Within the relevant range, SVOCs with lower values will equilibrate with the surface film more rapidly. Over time, the film becomes relatively enriched in species with higher  $\log K_{oa}$  values, while the proportion of gas-phase SVOCs not in equilibrium with the film decreases. Given stable airborne SVOC concentrations, films grow at faster rates initially, and then subsequently diminish to an almost steady growth rate. Once an SVOC is equilibrated with the film, its mass per unit film volume remains constant, while its mass per unit area increases in proportion to overall film thickness. The predictions of the conceptual model and its mathematical embodiment are generally consistent with results reported in the peer-reviewed literature.

**Keywords:** absorption, octanol/air partition coefficient, partitioning, semivolatile organic compounds, surface chemistry, window films

## Practical Implications

The relatively simple model of organic film growth presented in this paper can be used to better understand the evolution of organic films under a variety of indoor conditions. Better understanding of the composition of such films can support better estimates of SVOC exposures resulting from human contact with surface films. Also, organic films are expected to confer a degree of commonality among indoor surfaces with otherwise disparate chemical properties. Hence, the presence of films is anticipated to simplify the modeling of chemical transformations that are mediated by indoor surfaces.

## Introduction

Organic films are likely to be ubiquitous on indoor surfaces. This inference is based on the measured presence of numerous semivolatile organic compounds (SVOCs) at airborne concentrations in the 0.5 to 50 ppt range coupled with evidence regarding sorption and partitioning of gas-phase SVOCs to indoor surfaces.<sup>1-8</sup> The formation of such films and their existence on some indoor surfaces has been confirmed by both direct and indirect measurements.<sup>7-21</sup> Measurements also reveal that organic compounds are part of a larger array of species that contribute to total surface films indoors and outdoors. The additional species include water, water-soluble salts, other inorganic species and elemental carbon.<sup>21-22</sup> This paper is concerned with the organic portion of indoor surface films, emphasizing substrates that can be regarded as impermeable, such as windows.

The occurrence and growth of organic films on indoor surfaces influences the dynamic behavior of indoor SVOCs, serving as a sorptive reservoir. Furthermore, SVOCs present in surface films can be transferred to human skin via contact, with subsequent transdermal uptake of species that possess an appropriate set of physical-chemical properties.<sup>23</sup> Better understanding of organic film growth should improve estimates of human exposure to these compounds and aid in mitigating undesirable exposures.

Organic films also are expected to produce a degree of commonality among surfaces in a given indoor environment. Clean indoor surfaces differ from one another chemically. However, with exposure in indoor environments, they accumulate surface films. These films would tend to be similar both within and also across different occupied settings, since many of the constituents of indoor surface films are derived from the human occupants themselves (e.g., squalene, fatty acids, and other compounds found in skin oils), from occupant activities (e.g., cooking, cleaning) and from materials containing similar types of semivolatile additives

(e.g., plasticizers, flame-retardants, antioxidants). Such commonality in composition and governing processes potentially reduces the large range of different surface types that must be considered when evaluating indoor surface chemistry, and thereby potentially simplifies the modeling of chemical transformations that are mediated by indoor surfaces. Supporting this idea, a recent study by Wu et al.<sup>24</sup> found that, although the surface/air partition coefficients between DEHP and aluminum, polished glass and ground glass were substantially different when the surfaces were clean, the partition coefficients were similar when the surfaces were soiled.

Knowledge regarding organic films on indoor surfaces derives from a variety of studies. Many investigations have sampled window films, probing the rate at which organic films grow and quantifying the concentrations of selected organics in the film. This approach was pioneered by Diamond and colleagues<sup>11,15,21</sup> and has since been pursued by several other research groups.<sup>9,12-20</sup> Similar studies, under more controlled conditions, have been conducted in which windows, mirrors, glass plates and metal surfaces have been sampled after exposure in a chamber or a test house.<sup>10,25</sup> A different means of probing organic surface films has been to heat glass or metal surfaces that have been exposed for known periods to indoor air.

Thermal desorption is found to produce measurable ultrafine particles (UFP), from which one can infer the mass of SVOCs accumulated on the surface.<sup>7,8,26-28</sup> Surface wipes are yet another method by which information on indoor organic surface films has been obtained. For example, US EPA researchers measured the mass per unit area (i.e., the surface concentration) of more than 50 organic compounds in wipes of hard floors and food preparation surfaces in over 250 homes.<sup>29</sup> The resulting data have been used to estimate median values for organic film thicknesses on the sampled surfaces.<sup>23</sup> A final piece of evidence for indoor surface films comes from measurements of ozone deposition velocities in different indoor environments. Although ozone deposition velocities to different materials

that are commonly found indoors span five orders of magnitude when such materials are tested in experimental chambers,<sup>30-33</sup> the deposition velocities measured in different indoor environments span a relatively narrow range.<sup>32,34-36</sup> A potential explanation is a degree of commonality among indoor surfaces that is provided by the accumulated organic films.

These different experimental approaches probing organic films have produced congruent information that can be summarized as follows. The organic portion of indoor surface films commonly has an effective thickness between 5 and 30 nm,<sup>8,16,17,21</sup> depending on the nature of the indoor environment and how long the surface has been exposed to indoor air. The growth rate of organic films to clean surfaces is faster in the early period of growth and then slows over time; for periods of months, organic film growth is in the range 30-320  $\mu\text{g m}^{-2} \text{ d}^{-1}$  or 0.03-0.32  $\text{nm d}^{-1}$ .<sup>8,10,12,16,17,21</sup> The predominant organic constituents possess a relatively narrow range of octanol-air partitioning coefficients ( $K_{\text{oa}}$  values), relative to the much wider range of values for SVOCs found indoors.<sup>9,11,12,14,17,18,20</sup> For SVOCs with  $\log K_{\text{oa}} < 14$ , the concentrations of selected SVOCs measured simultaneously in the films and in the gas-phase are close to what would be anticipated from equilibrium partitioning theory.<sup>9,10,14,18,20</sup> The concentrations (mass per unit volume) of lower molecular weight SVOCs in organic films are relatively constant over time, whereas the concentrations of higher molecular weight SVOCs in surface films tend to increase over time.<sup>16,20</sup>

In what follows we strive to illuminate the dynamics of organic film formation, exploring the important emergent properties associated with the growth of such films on indoor surfaces. This paper has several specific aims: (1) to apply knowledge of the physical chemistry of SVOCs to construct a conceptual model of the dynamics of surface film growth focusing on uptake of gas-phase SVOCs with varying  $K_{\text{oa}}$  values; (2) to reconcile and

interpret what we know from experiments with knowledge of physical and chemical behavior of SVOCs; and (3) to add new insights to the collective scientific understanding of indoor surface film occurrence and growth.

A note is warranted on the terminology used throughout the paper when discussing organic surface films: *concentration* is used to quantify the mass of an SVOC or a group of SVOCs per volume of organic film; *surface concentration* is used to describe the analogous mass per area (i.e. per unit area of an impermeable substrate).

### **Envisioning the evolution of organic films on indoor surfaces**

Consider a room whose air contains SVOCs. If a clean, impermeable surface such as window glass is introduced into this room, how do the gas-phase SVOCs interact with this surface? Initially, some SVOCs would *adsorb* to the surface. Soon SVOCs will begin to *absorb* into the organics previously accumulated. As the sorption process proceeds, the thickness of this nascent surface film grows. The initial adsorptive process is envisioned to occur quickly, but to only form a thin layer, perhaps of the order of a monolayer thick ( $\sim 1$  nm). Subsequently, one can describe the process governing the absorption and growth of this organic film in terms of partitioning of SVOC species between the gas-phase and the surface film. Each SVOC in the room has a partition coefficient that describes the ratio of its equilibrium concentration in the surface film to its gas-phase concentration. In the discussion that follows, we will assume that the partition coefficient of each SVOC can be approximated by its octanol/air partition coefficient ( $K_{oa}$ ). In other words, we assume that octanol is a reasonable surrogate for the mix of organics that constitute the film, which would include a substantial proportion of oxidized compounds. We also assume that the surface film exhibits sorptive properties that are adequately approximated by bulk liquid octanol, even when the film is too thin to possess exactly the same thermodynamic properties as a bulk liquid.

Among the gas-phase SVOCs, those with lower  $K_{oa}$  values will equilibrate with the evolving surface film more rapidly and those with higher  $K_{oa}$  values will take longer to approach equilibrium. This process will be bounded, because airborne species with particularly high values of  $K_{oa}$  will partition preferentially to airborne particulate matter, depressing their gas-phase concentrations. In particular, for species with values of  $\log K_{oa}$  higher than approximately 12, partitioning into the airborne particle phase is preferred over the gas phase.<sup>5</sup> This feature slows the net rate of transport to indoor surfaces (except, perhaps, for those that are oriented upwards).

To put the partitioning time scales into perspective, consider these estimates. A compound with  $\log K_{oa}$  of 6 will approach equilibrium with respect to partitioning into an organic film of 5 nm thickness with a characteristic time of  $\sim 0.1$  minute. The equilibration time scale for a surface film scales linearly with the value of  $K_{oa}$ .<sup>5</sup> So, for a compound with a  $\log K_{oa}$  value of 10, the equilibration time scale will be on the order of  $10^4$  times as long, or 1000 minutes (= 16 hours). For the case of  $\log K_{oa} = 12$ , the equilibration time scale for absorptive partitioning from the gas phase will expand to  $10^5$  minutes ( $\sim 70$  days). The equilibration time scale also varies linearly with film thickness, so the time scales just reported would be increased by  $6\times$  for a film thickness of 30 nm rather than 5 nm.

Assume that the indoor gas- and particle-phase SVOC concentrations are relatively constant, maintained by processes that operate outside of partitioning to surface films, such as emissions from primary sources and removal by ventilation. Once an SVOC has equilibrated with the surface film, its concentration in the film would remain constant, yet the compound would continue to absorb into the film as the film thickness grows. Such growth would be promoted by the uptake of the gaseous species with higher  $\log K_{oa}$  values that have not yet equilibrated. Consequently, over time, the growth of the evolving film would be driven by the progressively smaller proportion of gas-phase SVOCs possessing higher  $\log K_{oa}$  values –



compounds that have not yet reached their equilibrium concentrations in the organic film.

Also, with increasing time, the threshold  $K_{oa}$  value differentiating those compounds in equilibrium with the film to those not yet equilibrated would increase.

Under the described conditions, the rate of film growth would tend to decrease with time. From the starting condition of an adsorbed monolayer, the thickness of the organic film (corresponding to the mass per unit surface area) would grow initially at its maximum rate as SVOCs across a full range of  $\log K_{oa}$  values contribute. However, as the fraction of gas-phase SVOCs in equilibrium with the film becomes progressively larger, the film's thickness grows at a progressively slower rate. The growth of the film is effectively self-limiting. Practically speaking, by the time all of the gas-phase SVOCs with  $\log K_{oa}$  less than approximately 13 have equilibrated with the surface film, the gas-phase concentration of the remaining SVOCs would have become so small as to contribute negligibly to further film growth over realistic time scales. Here, the idea of a "realistic time scale" is based on a comparison of equilibration time scales with expected surface renewal times in indoor air, which would be limited to less than a few decades.

In brief, we propose that organic film growth on impermeable surfaces is a time-dependent process that is controlled by the gas-phase concentration of SVOCs with  $K_{oa}$  values in a relatively small range (spanning approximately three orders of magnitude). In the sections that follow, we will more explicitly develop this model of organic film growth, explore several of its implications, and assess the extent to which its predictions agree with published empirical evidence regarding indoor organic surface films.

## Formulating a mathematical model for surface film growth

In this section, we describe a mathematical formulation of the growth and evolution of organic films on smooth, impermeable surfaces. The formulation is based on a blended treatment of SVOCs in which species can be modeled as individual SVOCs or clustered into aggregate groupings. The groupings are organized around a basis set of  $\log K_{oa}$  values; this treatment parallels the volatility basis set concept that has been developed for understanding the partitioning of airborne SVOCs between the gas and particle phases.<sup>37</sup>

The model accounts for the coupled dynamics of film growth combined with changes in the surface concentration (mass per film area) and volumetric concentration (mass per film volume) for SVOCs sorbed into the film. The model for film growth incorporates the following key assumptions. (1) The concentrations of the gas- and particle-phase SVOCs are maintained at constant values by processes that act independently of sorptive uptake. (2) Initially, the impermeable surface has a starting film of thickness  $X_o$ , which subsequently grows by uptake of the absorbing SVOCs. (3) The rate-limiting step is mass transfer from gas phase to the surface film. (4) The thermodynamic properties of the film do not vary with composition (i.e., they do not change as sorption proceeds).

A film growth model with  $n$  components (such as  $n$  bins of species clustered according to  $K_{oa}$  values) allows for the quantitative exploration of some self-assembly properties of film growth. These properties include (1) the predominance of species with intermediate  $K_{oa}$  values ( $\log K_{oa} \sim 10-13$ ); (2) progressive enrichment during film growth toward species with higher  $\log K_{oa}$  values within the predominant range; and (3) a decline over time in the rate of film growth, such that the rate of growth is markedly slower at time scales on the order of 100 days as compared with the first day.

To proceed, we describe a multicomponent system in which the SVOC species possessing similar values of  $K_{oa}$  are clustered into groups, with each group represented by a single  $K_{oa}$  value. For example, all of the SVOCs with  $\log K_{oa}$  values in the range 10 to 11 might be represented by a single species having a  $\log K_{oa}$  value of 10.5. We define  $n$  such groups and use the integer index  $i$  to designate the specific group under consideration. The following parameter definitions then apply:

$C_{gi}$  = gas-phase concentration of SVOC group  $i$  (mass per volume of air)

$C_{pi}$  = particle-phase concentration of SVOC group  $i$  (mass per volume of air)

$C_{ti}$  = total airborne concentration of SVOC group  $i = C_{gi} + C_{pi}$  (mass per volume of air)

$C_{fi}$  = concentration of sorbed SVOC group  $i$  in the film (mass per film volume)

$f_{om\_TSP}$  = volume fraction of organic matter in TSP

$M_{fi}$  = surface concentration of sorbed SVOC group  $i$  in the film (mass per film area)

$\rho_i$  = density of the condensed phase SVOC group  $i$  (mass per volume of SVOC group  $i$ )

$K_{oi}$  = equilibrium partitioning coefficient between sorbed SVOC and gas for group  $i$

$K_{pi}$  = particle-air partition coefficient for SVOC group  $i$  ( $\text{m}^3 \mu\text{g}^{-1}$ )

$v_{di}$  = deposition velocity of SVOC group  $i$  (length per time)<sup>5</sup>

$X$  = film thickness (length)

$X_o$  = initial film thickness (length)

TSP = total airborne suspended particle concentration (mass per volume)

$F_i$  = net flux of SVOC group  $i$  to the surface film (mass per area per time)

The flux variables  $F_i$  are modeled in this way:

$$F_i = v_{di} \left( C_{gi} - \frac{C_{fi}}{K_{oi}} \right) \quad (1)$$

Note that the surface concentration of sorbed SVOCs in the film,  $M_{fi}$ , can be expressed in terms of the film thickness and the SVOC concentrations in the film:

$$M_{fi} = X C_{fi} \quad (2)$$

It is convenient to select as primary variables  $M_{fi}$  and  $X$ , since the governing differential equations can be naturally written as rates of change of sorbed SVOC masses. Substitute equation (2) into the flux terms so that they are written in terms of  $M_{fi}$ :

$$F_i = v_{di} \left( C_{gi} - \frac{M_{fi}}{X K_{oi}} \right) \quad (3)$$

Now, one can write the material balance expression for the increase in film mass of a given component in this compact form for the multicomponent system:

$$\frac{d(M_{fi})}{dt} = F_i \quad (4)$$

The final equation needed to specify the system mathematically couples the film concentrations to the film thickness:

$$X = X_o + \sum_{i=1}^n \frac{M_{fi}}{\rho_i} \quad (5)$$

The numerical solution method marches forward in time by solving the system of  $i$  equations (4) for  $M_{f1}, M_{f2}, \dots, M_{fn}$ . At each step,  $X$  is updated using the algebraic equation (5).

The Supporting Information includes a spreadsheet that implements this model for five SVOC clusters over a time period of 500 days. The first cluster includes SVOCs with log  $K_{oa}$  values between 8 and 9, and is evaluated at the midpoint of the range (8.5). The clusters follow sequentially with the fifth cluster including SVOCs with log  $K_{oa}$  values between 12 and 13, evaluated at 12.5. The approach is generalizable to an arbitrary number of clusters. It is also amenable to a hybrid calculation in which one or more specific SVOCs are modeled individually even as other SVOCs in the surface film are simulated using the clustered basis-set approach.

### Self-assembly properties of indoor organic surface films

The mathematical model described in the previous section predicts a number of experimentally observed features of organic film growth on impermeable indoor surfaces. Using archetypical situations, this section illustrates key features captured by the model.

**Predominance of SVOCs with intermediate  $K_{oa}$  values.** It is instructive to begin by examining the distribution of organic compounds, as a function of their  $K_{oa}$  values, in surface films under equilibrium conditions. The gas-particle partitioning of SVOCs is modeled as previously described<sup>38</sup> and gas-surface film partitioning is assessed using the relationships described in the previous section. Consider SVOCs with log  $K_{oa}$  values between 7 and 14, grouped into seven SVOC clusters centered on log  $K_{oa}$  values 7.5, 8.5 ... 13.5. Assume that  $C_{ti}$  in each cluster is  $2.75 \mu\text{g}/\text{m}^3$ ,  $\text{TSP} = 20 \mu\text{g}/\text{m}^3$ ,  $f_{om\_TSP} = 0.4$ , the entire particle-phase of SVOC group  $i$  ( $C_{pi}$ ) participates in partitioning, and the thickness of the organic film is 10 nm. For these conditions, Figure 1 shows the mass per unit area of the organics present in the

film as a function of the  $\log K_{oa}$  values. The resulting plot exhibits a logistic-curve shape: there is negligible contribution of SVOCs with  $\log K_{oa} < 9$ ; there is a rapid increase in the mass per area over the range  $\log K_{oa} = 9$  to 13, and the curve levels off at values of  $\log K_{oa} > 13$ .

The relationship illustrated in Figure 1 assumes equilibrium conditions. However, long time scales are required for SVOCs with  $\log K_{oa}$  values much larger than 12 to attain equilibrium concentrations in a surface film. Also, the example illustrated in Figure 1 used equal values for  $C_{ii}$  in each cluster. However, SVOCs with  $\log K_{oa}$  values larger than 13 tend to be less abundant in indoor air than those with lower  $\log K_{oa}$  values.<sup>39-41</sup> Summarizing, for established surface films under typical indoor conditions, we anticipate that the organic constituents would be dominated by species with  $\log K_{oa}$  values between 10 and 13. Species with smaller  $\log K_{oa}$  values do not partition strongly to surface films from the gas phase; species with larger  $\log K_{oa}$  values have lower airborne concentrations and approach equilibrium slowly.

#### **Progressive enrichment of the film toward species with higher $\log K_{oa}$ values.**

How does the distribution of organic compounds, as a function of the  $\log K_{oa}$  values, change as a film evolves? We address this matter using the multicomponent model, considering SVOCs with  $\log K_{oa}$  values between 8 and 13. Specifically, we employ five clusters equally distributed on a log scale between  $\log K_{oa} = 8-9$  and  $\log K_{oa} = 12-13$ ; each cluster is modeled using the  $\log K_{oa}$  value at the center of its range. We ignore contributions of SVOCs with  $\log K_{oa} > 13$  because of the unrealistically long time scales for such SVOCs to contribute meaningfully to film growth. For the purposes of the first illustrative exercise, we assume that  $C_{ii}$  in each cluster is  $4 \mu\text{g}/\text{m}^3$ ,  $\text{TSP} = 20 \mu\text{g}/\text{m}^3$ ,  $f_{\text{om\_TSP}} = 0.4$ , and the initial thickness of the organic film is 2 nm. For these conditions, Figure 2a displays predicted film thickness versus time over a span of 500 days, at which time the film thickness would have grown from 2 nm

to 9 nm, and the surface concentrations would be 11, 110, 900, 3100 and 2900  $\mu\text{g m}^{-2}$  for five SVOC clusters centered on  $\log K_{\text{oa}}$  values of 8.5, 9.5, 10.5, 11.5 and 12.5, respectively. It is noteworthy that the mass distributions in the early periods of film growth are quite different than at the end of the modeled period. In the first few days, the film is dominated by the SVOC cluster with  $\log K_{\text{oa}}$  values of 10-11; at 4 days, the dominant SVOC cluster has  $\log K_{\text{oa}}$  values of 11-12; and, at 100 days, the SVOC cluster with  $\log K_{\text{oa}}$  values of 12-13 is more abundant than that with  $\log K_{\text{oa}}$  values of 10-11, but still less abundant than that with  $\log K_{\text{oa}}$  values of 11-12.

In the preceding example, we assumed that the airborne SVOC concentration,  $C_{ti}$ , has the same value in each cluster. However, as already noted, in typical indoor environments the value for  $C_{ti}$  is likely to be smaller for clusters with larger  $\log K_{\text{oa}}$  values. There are insufficient published data to reliably choose representative  $C_{ti}$  values for each of the  $\log K_{\text{oa}}$  clusters. However, one specific constraint must be satisfied: the values chosen for TSP and  $f_{\text{om\_TSP}}$  place an upper limit on the sum of  $C_{pi}$  in the clusters, which cannot exceed the product of  $f_{\text{om\_TSP}} \times \text{TSP}$ . The sum of  $C_{pi}$  in the clusters can be less than the product of  $f_{\text{om\_TSP}} \times \text{TSP}$  if some of the organic matter in TSP is effectively nonvolatile (e.g., being polymeric or oligomeric). The influence of the values chosen for  $C_{ti}$  is indicated by a second illustrative example in which the targeted SVOCs have  $\log K_{\text{oa}}$  clusters centered on 8.5, 9.5, 10.5, 11.5 and 12.5, and the respective values for  $C_{ti}$  are 20, 15, 10, 5 and 2  $\mu\text{g/m}^3$ . As before, we assume  $\text{TSP} = 20 \mu\text{g/m}^3$ ,  $f_{\text{om\_TSP}} = 0.4$ , and the initial thickness of the organic film is 2 nm. For these conditions, Figure 2b shows that the film thickness grows to 14 nm over a span of 500 days. As was the case in Figure 2a, the percentage of SVOCs with higher  $\log K_{\text{oa}}$  values increases as the film grows. However, since the present example weights  $C_{ti}$  towards SVOCs with lower  $\log K_{\text{oa}}$  values, the relative contributions to the film of SVOCs with  $\log K_{\text{oa}}$  values of 12-13 is smaller, while that of SVOCs with  $\log K_{\text{oa}}$  values of 9-11 is larger. Also note that

SVOCs with  $\log K_{oa}$  values of 8-9 still make only a small contribution to the organic film, even though their  $C_{ti}$  value is  $5\times$  larger ( $20$  vs.  $4\text{ }\mu\text{g}/\text{m}^3$  in the second case compared with the first).

**Kinetics of film growth.** Although the total SVOC concentration, its distribution as a function of  $\log K_{oa}$ , and the resulting final film thickness are different in Figures 2a and 2b, the film growth curves exhibit qualitatively similar shapes. In each case, the film grows at a faster rate in the initial days and subsequently grows at a diminished and almost constant rate over time scales on the order of a hundred days. The values chosen for airborne SVOC concentration in each of the five clusters,  $C_{ti}$ , influences the rate of film growth as well as the final film thickness. The influence of  $C_{ti}$  is greatest in  $\log K_{oa}$  clusters centered at 11.5 and 12.5, while the influence of  $C_{ti}$  in the lower two clusters (centered at 8.5 and 9.5) is relatively small. This outcome occurs because, in slightly more than 4 days, SVOCs with  $\log K_{oa}$  values of 8-10 would have reached equilibrium concentrations in the surface film and would remain in equilibrium with the growing film. In roughly 40 days, depending on the values for  $C_{ti}$ , SVOCs with  $\log K_{oa}$  values of 10-11 would have attained equilibrium concentrations in the surface film. For a reasonable range of indoor concentrations, SVOCs with  $\log K_{oa}$  values of 11-12 would reach equilibrium concentrations with the surface film in 300-500 days. Hence, after the first 4 days, film growth is driven primarily by sorption of SVOCs with  $\log K_{oa}$  values of 10-12, and after 40 days, by SVOCs with  $\log K_{oa}$  values of 11-13. Once an SVOC has reached its equilibrium concentration in the surface film, its concentration (mass per unit volume of film) remains constant, while its surface concentration (mass per unit area) increases as the film grows. The larger the total airborne concentrations of SVOCs in the  $\log K_{oa}$  range 11–13, the thicker the resulting organic film and the longer the time to equilibrium, since time to equilibrium scales with film thickness.<sup>5</sup>



**Accumulation of specific SVOCs in surface films.** Studies have also measured the evolving concentration of individual SVOCs in surface films (e.g., Figure S3b in Bi et al.<sup>10</sup>; Figure 3 in Huo et al.<sup>16</sup>). In addition to predicting overall time-dependent film growth and the distribution of SVOCs with various  $K_{oa}$  values in the evolving film, the model presented in this paper can be used to predict such individual SVOC evolution. To illustrate, a hybrid calculation is performed in which an SVOC is modeled individually while other airborne SVOCs are processed using clustered log  $K_{oa}$  values. The first “bin” of the model,  $C_{tl}$ , represents the total concentration of the SVOC in question and log  $K_{oa1}$  is the log  $K_{oa}$  value of the targeted SVOC. The four remaining “bins” represent log  $K_{oa}$  clusters centered at 9.5, 10.5, 11.5 and 12.5 and, in this example, have respective values for  $C_{ti}$  of 15, 10, 5, and 2  $\mu\text{g m}^{-3}$  (the same values used in the example presented in Figure 2b). We have performed this exercise for two brominated flame retardants commonly found indoors: BDE-47 and BDE-99 with respective log  $K_{oa}$  values of 10.2 and 11.3 at 25 °C.<sup>42</sup> We have assumed that their total airborne concentrations are 52 and 15  $\text{pg/m}^3$ , respectively; these are comparable to median airborne values reported in Venier et al.<sup>20</sup> Figure 3 displays the modeled results for the net accumulation of BDE-47 and BDE-99 in the organic surface film as it evolves over a 500-day period. In general tendency, the modeled results are consistent with results for individual SVOCs reported in the literature.<sup>10,16</sup> In the case of BDE-47, the initially elevated growth rate slows quickly and becomes almost constant after about 4 days, with the subsequent growth driven by the accumulation of material in the total organic film. In the case of BDE-99, the initial growth is not as fast as that of BDE-47, and the subsequent growth rate more slowly approaches a steady value driven by growth of the total organic film. We stress that these are only illustrative examples; results would depend on the actual SVOC concentrations in the log  $K_{oa}$  clusters centered at 9.5, 10.5, 11.5 and 12.5.

## Comparing model predictions with published results

Table 1 summarizes results from peer-reviewed studies relevant to the formation and growth of organic films on impermeable indoor surfaces. Most of these studies are based on sampling from window films; with one exception,<sup>4</sup> we only report results from *indoor* window films. One of the studies also includes samples of films from glass plates and mirrors in a test house<sup>10</sup> and two studies are based on particle measurements following thermal desorption of surface films on impermeable surfaces exposed to indoor air for different intervals.<sup>7,8</sup> Results from these studies can be used to explore the validity of predictions derived from the model.

**Table 1.** Studies related to organic films on impermeable indoor surfaces.

Study	Location	Surfaces and collection sites	Focus
Bennett et al. 2015 <sup>9</sup>	California	Windows and floors in 139 homes. Part of US EPA SUPERB study.	PBDEs
Bi et al. 2015 <sup>10</sup>	Austin, TX	Windows, plates and mirrors in UT Austin test house under two conditions: 21 °C and 30 °C.	Phthalates
Butt et al. 2004 <sup>11</sup>	Greater Toronto	Windows at bookstore, urban homes, urban and rural offices and electronics recycling facility.	PBDEs
Cetin and Odabasi, 2011 <sup>12</sup>	Izmir, Turkey	Windows in suburban university, five urban homes, urban TV shop, a rural site and an industrial site.	PBDEs
Duigu et al. 2009 <sup>13</sup>	Brisbane, Australia	Windows in eighteen suburban bungalows, apartments and townhouses.	PAHs
Gao et al. 2016 <sup>14</sup>	Beijing	Windows at nine homes, four dormitories and six offices 3 months or more after cleaning.	Chlorinated paraffins
Gerwurtz et al. 2009 <sup>15</sup>	Greater Toronto	Windows in two downtown, three suburban, and two rural buildings.	Perfluoroalkyls
Huo et al.	Harbin, China	Windows in two university buildings sampled	Phthalates

2016 <sup>16</sup>		at 7-day intervals in winter and summer	
Li et al. 2010 <sup>17</sup>	Guangzhou Hong Kong	Windows in three university offices and three homes in Guangzhou; six university offices and three homes in Hong Kong	PBDEs
Liu et al. 2003 <sup>21</sup>	Greater Toronto	Windows in rural office/lab, suburban office building and five urban homes sampled 3-5 months after cleaning.	<i>n</i> -Alkanes, mono-di-, aromatic- and terpene-acids
Melymuk et al. 2016 <sup>18</sup>	Brno, Czech Republic	Windows from a residential bedroom over 28 days in March and April 2013.	PCBs, OCPs, PBDEs, NFRs, PAHs
Pan et al. 2012 <sup>19</sup>	Guangzhou Hong Kong	Windows in three university offices and three homes in Guangzhou; six university offices and three homes in Hong Kong	PAHs
Venier et al. 2016 <sup>20</sup>	Bloomington, Toronto  Brno	Windows from 20 US, 23 Canadian and 20 Czech residences. Samples from bedroom in each and living room in ~ half the homes.	BFRs
Wallace et al. 2015 <sup>7</sup>	Palo Alto Redwood City	Stainless steel pans, previously cleaned by heating, exposed 5 – 300 h in Palo Alto and up to 1800 h in Redwood City.	SVOCs
Wallace et al. 2017 <sup>8</sup>	Palo Alto Redwood City Hong Kong	Petri dishes and aluminum foils exposed in homes in California and a lab in Hong Kong for periods ranging from 1 hour to 281 days.	SVOCs
Wu et al. 2008 <sup>4</sup>	Toronto Dorset, Ont.	Glass beads located outdoors but protected from precipitation.	PCBs

<sup>a</sup> Abbreviations: BPA: bisphenol A; OCPs: organochlorine pesticides; PAHs: polycyclic aromatic hydrocarbons; PBDEs: polybrominated diphenyl ethers; BFRs: brominated flame retardants; PCBs: polychlorinated biphenyls; NFRs: novel halogenated flame retardants.

**Partitioning and predominance of SVOCs with intermediate  $K_{oa}$  values.** Several studies in Table 1 have reported measured concentrations of individual SVOCs in organic surface films and examined how these concentrations relate to their respective air concentrations. Based on air samples and surface wipes of windows and floors in 139

northern and central California homes, Bennett et al.<sup>9</sup> found that concentrations of BDE-47 and -99 in air were strongly correlated ( $r > 0.5$ ,  $p < 0.001$ ) with those in window films; BDE-153 and -154 in window films were also strongly correlated with concentrations in floor wipes. Bi et al.<sup>10</sup> exposed plates and mirrors in a test house at two carefully controlled temperatures: 21 °C and 30 °C. The authors measured butyl benzyl phthalate (BBzP) and di(2-ethylhexyl) phthalate (DEHP) concentrations in the air and surface-concentrations on the exposed materials. Using an estimated film thickness and fractional organic content, they calculated partitioning coefficients for the windows, plates and mirrors at the two temperatures. These partitioning coefficients were similar to  $K_{oa}$  values for BBzP and DEHP at 21 °C and 30 °C. Gao et al.<sup>14</sup> found that, for a series of short-chain chlorinated paraffins (SCCPs), the C10 and C11 congeners, with calculated  $\log K_{oa}$  values between 9 and 11, were the most abundant SCCPs in surface films. Partitioning between organic films and air scaled with the calculated  $K_{oa}$  values of the SCCPs. However, predicted gas-phase concentrations based on concentrations in films tended to be larger than measured gas-phase concentrations, perhaps reflecting estimated  $K_{oa}$  values that did not properly align with the mix of isomers in each formula group. Melymuk et al.<sup>18</sup> observed that, after 28 days, mass fractions of lower molecular weight polybrominated diphenyl ethers (PBDEs) and polycyclic aromatic hydrocarbons (PAHs) in films tended to scale with respective concentrations in air. High molecular weight compounds did not appear to be in air/surface film equilibrium. Furthermore, gas-phase concentrations of legacy SVOCs were more likely to be in equilibrium with surface films than was the case for emerging SVOCs. Venier et al.<sup>20</sup> reported that concentrations in air, mass-fractions in dust and surface-concentrations in window films were significantly correlated for about twenty brominated flame retardants (BFRs). Window-film/gas-phase partition coefficients increased with increasing  $K_{oa}$  for BFRs with  $\log K_{oa} < 14$ , but not for those with  $\log K_{oa} > 14$  (see Fig. 5 of cited paper).

The most abundant PBDEs in window films tend to be BDE-47, -99, -100, -153, -154 and -209;<sup>9,11,12,17,18,20</sup> these PBDEs have log  $K_{oa}$  values in the range of 10.2 to 12.9.<sup>42</sup> The presence of BDE-209 in window films does not appear to be consistent with a partitioning model of the type used in this paper, since it is anticipated to have a very high  $K_{oa}$  value and to be present almost exclusively in the particle phase (although appreciable gas-phase concentrations of BDE-209 have been reported<sup>12</sup>). This observation suggests that processes other than gas-to-surface film partitioning may also contribute to SVOCs found in surface films, especially for SVOCs with large  $K_{oa}$  values such that they are predominately partitioned to particles when airborne. (See section entitled *What about particles?*)

Taken together, the above results largely support the formulation of the current model, including its predictions regarding the range of  $K_{oa}$  values associated with the most abundant SVOCs in surface films.

**Progressive enrichment of the film toward species with higher log  $K_{oa}$  values.** Wu et al.<sup>4</sup> measured the proportion of various PCB congeners in films growing outdoors on sheltered glass beads over a period of 273 days. In the early stages of film growth, the di- to tetra-PCBs accounted for up to 70% of the total mass of PCBs in the film. At the end of the study periods, the penta- to deca-PCBs dominated the total PCBs, while the di- to tetra-PCBs accounted for roughly 10% of the total PCB mass. Although these results are complicated by changes in outdoor temperature during the study period, temperature changes alone do not explain the evolution of PCB composition towards the congeners with higher log  $K_{oa}$  values. Pan et al.<sup>19</sup> measured polycyclic aromatic hydrocarbons (PAHs) in the same window film samples from Guangzhou and Hong Kong that had been part of an earlier study of PBDEs in window films.<sup>17</sup> For indoor window films, they reported that the growth rates of PAHs with lower  $K_{oa}$  values (“light-weight” PAHs in their terminology) were initially fast and then approached a constant level. In contrast, the growth rates of PAHs with higher  $K_{oa}$  values

(“heavy-weight” PAHs) displayed nearly linear growth over a 40-day period. Huo et al.<sup>16</sup> in their study of window films within university buildings in Harbin, China, found that the surface-concentrations of DEHP ( $\log K_{oa} \sim 12.9$ ), BBzP ( $\log K_{oa} \sim 11.6$ ) and di(*n*-butyl) phthalate (DnBP,  $\log K_{oa} \sim 9.8$ ) in indoor window films exhibited strong growth over the 49 (winter) and 77 (summer) day study periods. Conversely, the surface-concentrations of diethyl phthalate (DEP,  $\log K_{oa} \sim 8.2$ ) and dimethyl phthalate (DMP,  $\log K_{oa} \sim 7.5$ ) did not increase over time. That is, in both the Pan et al.<sup>19</sup> and the Huo et al.<sup>16</sup> studies, surface films tended to become enriched over time in SVOCs with higher  $\log K_{oa}$  values relative to those with lower  $\log K_{oa}$  values.

**Kinetics of film growth.** Studies by Liu et al.,<sup>21</sup> Li et al.,<sup>17</sup> Bi et al.,<sup>10</sup> Gao et al.,<sup>14</sup> and Wallace et al.<sup>8</sup> have reported rapid initial growth followed by slower and more constant growth of organic films on indoor surfaces. Table 2 summarizes measured rates of organic film growth on indoor surfaces reported in the literature.

**Table 2.** Rates of organic film growth on indoor surfaces reported in published literature.

Study	Film thickness (nm)	Duration (d)	Growth rate (nm d <sup>-1</sup> )
Liu et al. <sup>21</sup>	Mean: 5	90-150	0.03 – 0.06
Li et al. <sup>17</sup>	Guangzhou: 4.2-13 Hong Kong: 1.4-9.4	40	Guangzhou: 0.11 – 0.32 Hong Kong: 0.04 – 0.24
Huo et al. <sup>16</sup>	Winter mean: 8.4 Summer mean: 14	Winter: 49 Summer: 77	Winter mean: 0.17 Summer mean: 0.18
Gao et al. <sup>14</sup>	GM: 13 <sup>a</sup>	> 90	GM < 0.14
Wallace et al. <sup>8</sup>	Best fit: 10 <sup>b</sup> Best fit: 18 <sup>b</sup>	50 100	Best fit: 0.20 Best fit: 0.18

	Best fit: 26 <sup>b</sup>	200	Best fit: 0.13
	Best fit: 29 <sup>b</sup>	281	Best fit: 0.10

<sup>a</sup> Total film thickness (organic and inorganic constituents) calculated from film masses assuming a density of 1.7 g cm<sup>-3</sup>. GM = geometric mean. <sup>b</sup> Petri dishes and foils exposed horizontally for up to 281 days. Values in table calculated from two-parameter fit of measured mass emitted per cm<sup>2</sup>.

At sites in greater Toronto, researchers from the Diamond group made the first measurements of organic films on indoor windows.<sup>21</sup> After 3 to 5 months the average thickness of organic films in indoor rural and suburban homes was 5 nm, indicating a growth rate of about 0.03 – 0.06 nm d<sup>-1</sup>. Of the classes of organic compounds analyzed (*n*-alkanes, monoacids, diacids, aromatic acids, and terpene acids), monoacids were the most abundant, particularly palmitic acid. This finding may reflect the influence of human occupants, since palmitic acid is the most abundant fatty acid in human skin surface lipids, accounting for 25% of skin oil's total fatty acids.<sup>43</sup> In the Li et al. study<sup>17</sup> it was reported that, after 40 days, the thickness of organic films on indoor windows was in the range 4–13 nm (geometric mean ~ 8 nm) in Guangzhou and 1–9 nm (geometric mean ~ 6 nm) in Hong Kong, assuming a film density of 0.83 g cm<sup>-3</sup> and an organic matter/organic carbon ratio of 1.6 (see Fig. 1 of cited paper). This evidence corresponds to a growth rate of 0.11–0.32 nm d<sup>-1</sup> in Guangzhou and 0.04–0.24 nm d<sup>-1</sup> in Hong Kong. For sites in Harbin, Huo et al.<sup>16</sup> reported mean surface film thicknesses of ~ 8 nm after 49 days of growth in the winter and 14 nm after 77 days of growth in the summer. These resulting thicknesses correspond to average growth rates of ~ 0.2 nm/day for overall film growth; rates for the organic portion of the film are expected to be smaller. Based on measurements at 19 sites in Beijing, Gao et al.<sup>14</sup> reported a geometric mean organic film surface concentration of 13 mg/m<sup>2</sup> (equivalent to a thickness of 13 nm assuming

a film density of  $1.0 \text{ g cm}^{-3}$ ). They stated that the windows had not been cleaned for at least 3 months prior to sampling, indicating an upper-bound average growth rate of  $0.15 \text{ nm d}^{-1}$  for the organic films on these Beijing buildings. Wallace et al.<sup>8</sup> exposed Petri dishes and sheets of aluminum foil to air in a home office for intervals ranging from 1 to 281 days. Thermal desorption of these surfaces produced ultrafine particles that were quantified in different size-fractions. Assuming that all of the mass associated with the measured particles was from SVOCs sorbed to the dish or foil surfaces and a film density of  $1.0 \text{ g cm}^{-3}$ , organic film growth occurred at a rate of approximately  $0.18 \text{ nm d}^{-1}$  based on a linear fit to the measurements over the first 108 days. The linearized average growth rate ranged from  $0.21 \text{ nm d}^{-1}$  at 50 days to  $0.10 \text{ nm d}^{-1}$  at 281 days based on the modeled fit in Figure 2 of the cited paper. These surfaces were exposed horizontally and, although visible dust was removed with a puff of air prior to heating, settled coarse particles may have contributed to the desorbed organics.

The estimated growth rates, for the conditions modeled in Figure 2b, are  $0.08 \text{ nm d}^{-1}$  at 100 days and a little more than  $0.05 \text{ nm d}^{-1}$  at 200 days. The environmental conditions modeled to generate Figure 2b (e.g., values of TSP and  $C_{ti}$ ) are expected to be more like those in greater Toronto<sup>21</sup> than those of study locations in China<sup>14,16,17</sup>. The indoor sites in China are anticipated to have higher TSP and higher total SVOC concentrations than the Toronto sites, resulting in faster film growth. That said, it should be noted that the film-growth process is somewhat buffered against the influence of increases in TSP and total airborne concentration of SVOC groups,  $C_{ti}$ . All else being equal, as TSP increases, the fraction of SVOCs in the gas-phase decreases. A smaller fraction in the gas-phase reduces the influence of increased SVOC concentration within a given  $\log K_{oa}$  cluster. This feature may partially explain why the growth rates cited above are as similar as they are, despite being measured at different locations.



## What about particles?

At what rates do particles contribute to the growth of organic films on indoor surfaces? The flux of particles to indoor surfaces, equivalent to the rate at which particle mass accumulates on indoor surfaces per unit surface area, can be expressed as follows:

$$F_{\text{part}} = C_p \times v_d \quad (6)$$

where  $C_p$  is the indoor particle concentration ( $\mu\text{g}/\text{m}^3$ ) and  $v_d$  is the mean deposition velocity (m/h) for these particles. Equation 6 neglects processes such as resuspension that result in particle loss from surfaces. When considering airborne mass, it is convenient to cluster particles into two size modes: fine-mode particles ( $< 2.5 \mu\text{m}$  aerodynamic diameter) and coarse-mode particles ( $> \text{than } 2.5 \mu\text{m}$  diameter). The indoor concentration of coarse-mode particles is substantially influenced by occupancy, since resuspension from contact surfaces and emissions from the occupants themselves are important sources of airborne coarse particles.

Table 3 summarizes estimates that are detailed in the Supporting Information of fine- and coarse-mode particle contributions to total mass as well as organic matter on vertical and horizontal surfaces. For vertical surfaces, in the absence of thermophoresis, fine- and coarse-mode particles are anticipated to make similar contributions to the accumulation of organic matter – in the range of 0.3 to 3  $\mu\text{g}/(\text{m}^2 \text{ d})$ . In Table 2, absorption of gas-phase organics to indoor impermeable surfaces, regardless of orientation, was reported to be in the range of 30 to 330  $\mu\text{g}/(\text{m}^2 \text{ d})$  assuming that 1  $\text{mg}/(\text{m}^2 \text{ d}) \sim 1 \text{ nm d}^{-1}$ . Hence, on vertical surfaces, the accumulation of organic matter via particle deposition is expected to occur at rates one to four orders of magnitude slower than those resulting from the absorption of gas-phase SVOCs. During cold weather, thermophoresis might be the dominant fine-mode particle transport mechanism for delivery to window surfaces, but even then the estimated

accumulation rates for organic matter from fine-mode particles is only a small fraction of that anticipated from absorption of gas-phase SVOCs. For upward horizontal surfaces, coarse-mode particles are anticipated to be substantially more important than fine-mode particles for the delivery of organics. The accumulation of organic matter on top-facing horizontal surfaces via deposition of coarse-mode particles appears to occur at rates ( $20\text{--}9000\text{ }\mu\text{g}/(\text{m}^2\text{ d})$ ) that are comparable at the lower end and larger at the upper when compared with the corresponding range for absorption of gas-phase organics ( $30\text{--}330\text{ }\mu\text{g}/(\text{m}^2\text{ d})$ ).

Hence, these estimates indicate that, under typical indoor conditions and for the first several hundred days, the growth of organic films on vertically oriented indoor surfaces should be dominated by absorption of gas-phase SVOCs. However, for topside horizontal surfaces, absorption of SVOCs and deposition of coarse-mode particles both contribute significantly to organic film growth. As the time of exposure extends beyond a year, we anticipate that partitioning from the gas-phase would contribute progressively less and deposition of particles would therefore contribute proportionally more to the growth of organic films on indoor surfaces. Whether partitioning from the gas-phase continues to dominate at these time scales depends on the gas-phase concentration of SVOCs with  $\log K_{oa} > 12$ , as well as on the airborne concentration of fine- and coarse mode particles and the fraction of organic matter in these particles.

**Table 3.** Accumulation of mass and organic matter on vertical and topside horizontal surfaces as a consequence of particle deposition (see Supporting Information for references and assumptions).

	<b>Deposition velocity (<math>v_d</math>),</b> m/h	<b>Total mass accumulation rate,</b> $\mu\text{g}/(\text{m}^2 \text{ d})$	<b>Organic matter accumulation rate,</b> $\mu\text{g}/(\text{m}^2 \text{ d})$
<b>Vertical surfaces</b>			
Fine-mode particles	0.002 (median) 0.004 (max)	0.5 – 2	0.2 – 1
Fine-mode particles with thermophoresis	0.02	5 – 10	3 – 5
Coarse-mode particles	0.016 – 0.043	0.4 – 15	0.8 – 3
<b>Topside horizontal surfaces</b>			
Fine-mode particles	0.04 (median)	10 – 20	5 – 10
Coarse-mode particles	5 – 30	120 – 11,000	20 – 2200
Human emissions (particles > 1.0 $\mu\text{m}$ )	—	$170 \pm 100$	$20 \pm 10$
Dustfall	—	3000 – 43,000	600 – 9000

### Additional considerations and future outlook

Within a critical range, modeled results are sensitive to the specific  $K_{\text{oa}}$  values. For example, we have indicated in this work that the key range for film growth onto vertically oriented impermeable indoor surfaces spans log  $K_{\text{oa}}$  values between 10 and 13. It is difficult to measure  $K_{\text{oa}}$  at such high values; uncertainties in measured or calculated  $K_{\text{oa}}$  values tend to be large.<sup>44</sup> This feature, in turn, leads to large uncertainties in model predictions of partitioning between the gas-phase and a surface film. For example, consider a hypothetical SVOC whose total airborne concentration is  $0.2 \mu\text{g m}^{-3}$ , while the total airborne

concentrations of SVOC clusters are  $C_{ti} = 15, 10, 5$  and  $2 \mu\text{g m}^{-3}$ , respectively, for  $\log K_{oa}$  bins centered at 9.5, 10.5, 11.5 and 12.5; initial film thickness = 2 nm; TSP =  $20 \mu\text{g m}^{-3}$ ; and  $f_{om\_TSP} = 0.4$ . Assume that its  $\log K_{oa}$  value is  $11.0 \pm 0.5$  at room temperature. If the actual value of  $\log K_{oa}$  is 10.5, then its predicted surface-concentration after 100 days is  $40 \mu\text{g m}^{-2}$ ; if the actual value of  $\log K_{oa}$  is 11.5, then its predicted surface-concentration is  $125 \mu\text{g m}^{-2}$ . Consequently, for these conditions, uncertainty in the  $\log K_{oa}$  value of  $\pm 0.5$  translates to uncertainty in the predicted surface concentration spanning a factor of three. Below and above the critical  $K_{oa}$  range, the predictions of mass/area and mass/volume of surface films are less sensitive to uncertainty in  $K_{oa}$  values.

There are no reported measurements of the distribution of total airborne concentrations of SVOCs in an indoor environment as a function of their  $K_{oa}$  values. In the modeling examples conducted in this paper, it was necessary to estimate the total concentration of indoor SVOCs in each of the  $\log K_{oa}$  size-bins using either educated guesses<sup>37</sup> or incorporating information from limited measurements<sup>45</sup> of the loadings of organic mass distributed according to their mass-equivalent effective saturation concentration obtained in an outdoor sampling campaign, coupled with reported concentrations of SVOCs in various indoor environments.<sup>39-41</sup> The latter data tend to be restricted to relatively nonpolar SVOCs that are easily measured using conventional GC/MS techniques. More polar SVOCs such as mono- and dicarboxylic acids and compounds with mixed functional groups are missed in such surveys. It is only recently that state-of-the-art techniques have started to be applied to the measurement of such SVOCs in indoor air.<sup>46,47</sup> Applying approaches similar to those described in Cappa and Jimenez<sup>45</sup> to indoor organic surface films could yield important information regarding the volatility distribution of the compounds that constitute such films.

Reactions in the gas-phase between oxidants (e.g., O<sub>3</sub>, NO<sub>3</sub>•, OH•, Criegee intermediates) and indoor organic compounds generate products with a range of volatilities. The less volatile of these products contribute to the formation and growth of secondary organic aerosol. We anticipate that many of these same products will contribute to the growth of indoor surface films. Oxidation reactions are also anticipated to occur at the air-surface interface and within surface films. The present model formulation does not include such reactions. It also ignores other chemical transformations that are likely to occur in surface films. These include hydrolysis reactions and acid/base reactions, as well as dimerization/oligomerization reactions analogous to those reported to occur in secondary organic aerosol.<sup>48</sup> Many of the oxidation and hydrolysis products are expected to redistribute between the film and the gas-phase. Dimerization and oligomerization products have very low vapor pressures, which effectively lock these products into the surface film – they become chemical compounds that do not participate in redistribution via partitioning. Oxidation and dimerization/oligomerization may also change the phase state of organic surface films, altering their viscosity. This process would, in turn, influence diffusion within organic films. To provide some perspective, note that diffusion coefficients are up to a factor of 10<sup>7</sup> smaller in highly viscous organic matter as compared to in organic liquids.<sup>49</sup>

Surface films have constituents in addition to organic matter; among these is water. The water content of surface films depends in part on the type and concentration of water-soluble salts present in the film and also on the humidity of the indoor environment referenced to the surface temperature. Both humidity levels and surface temperatures can vary substantially over relatively short time scales (hours) and both often vary diurnally, resulting in concomitant variations in the water content of the surface films. Hence, the surface film can swell or shrink with changing moisture conditions. When the water content of a surface film is elevated, a somewhat structured layer of surface-active organic molecules

might form at the air-interface of the film.<sup>49,50</sup> Such a structured layer is anticipated to impede the transport of molecules into and out of the overall surface film. The present model does not address such features and their importance cannot be evaluated from the present state of knowledge.

This paper has considered the formation and growth of organic films on smooth, impermeable indoor surfaces (e.g., window glass and metal objects). However, many indoor surfaces are fibrous, permeable or semi-permeable. Prominent examples are carpets, upholstered furniture, bedding, clothing, wood products and painted walls. In future work, the ideas presented in this paper might be usefully extended to such surfaces. Important attributes to consider are the influence of the chemical composition of the substrate, the porosity, and the surface topography on partitioning in relation to the formation of surface films. Insights regarding SVOC partitioning to polymeric coatings (e.g., paints, varnishes, lacquers, vinyl wall coverings) and polymeric materials may also be gained from studies of gas-wall partitioning in Teflon bags commonly used as reaction chambers by atmospheric chemists. There exists a substantial body of work in this area, as summarized by Krechmer et al.<sup>52</sup> In contrast to results reported for organic films on impervious indoor surfaces, Krechmer et al. measured timescales for equilibrium to the Teflon walls of their chamber that were on the order of 10 minutes. They interpret their results as partitioning of SVOCs into a thin Teflon film (effective thickness  $\leq 1.5$  nm) instead of into an evolving organic film such as that encountered on an impermeable indoor surface.

In summary, the evolution of an organic film on indoor surfaces depends on three important factors: the concentrations of the SVOCs in indoor air, the  $K_{oa}$  values for these SVOCs, and time. The SVOCs that most contribute to the organic surface films are those whose product of concentration and partitioning coefficient (approximated here as  $K_{oa}$ ) are largest. Regarding time, SVOCs with lower  $K_{oa}$  values equilibrate faster; higher  $K_{oa}$  species

equilibrate more slowly. The slow approach to equilibrium for the species with intermediate and larger  $K_{oa}$  values controls film growth over a period of months and years. The model that we have presented enables quantitative estimates and predicts qualitative features that agree well with published empirical evidence from several research groups. Our collective understanding about the prevalence, composition, and dynamic behavior of organic surface films can help orient future research efforts to better understand human exposure to semivolatile organic compounds in indoor environments. For example, the model implies that frequent cleaning of exposed indoor surfaces can reduce indoor exposures to SVOCs, especially those with  $\log K_{oa}$  values between 9 and 12. Such cleaning – if effective in removing surface films – would reduce dermal absorption following contact with contaminated surfaces and is also expected to reduce inhalation intake, since cleaning would increase the average flux of SVOCs to surfaces thereby lowering airborne SVOC concentrations. Additionally, knowledge regarding the prevalence, composition, and dynamic behavior of organic surface films can result in better understanding of surface-mediated indoor chemistry.

### **Supporting Information**

Additional Supporting Information, including estimates of fine- and coarse-mode particle contributions to organic matter on vertical and horizontal surfaces and a table showing approximate relationships between  $K_{oa}$ , saturation vapor pressure, and saturation concentration, may be found online in the supporting information tab for this article.

## References

1. Law NL, Diamond ML. The role of organic films and the effect on hydrophobic organic compounds in urban areas: An hypothesis. *Chemosphere*. 1998;36:2607-2620.
2. Diamond ML, Priemer DA, Law NL. Developing a multimedia model of chemical dynamics in an urban area. *Chemosphere*. 2001;44:1655-1667.
3. Wu RW, Harner T, Diamond ML, Wilford B. Partitioning characteristics of PCBs in urban surface films. *Atmos Environ*. 2008;42:5696-5705.
4. Wu RW, Harner T, Diamond ML. Evolution rates and PCB content of surface films that develop on impervious urban surfaces. *Atmos Environ*. 2008;42:6131-6143.
5. Weschler CJ, Nazaroff WW. Semivolatile organic compounds in indoor environments. *Atmos Environ*. 2008;42:9018-9040.
6. Csiszar SA, Diamond ML, Thibodeaux LJ. Modeling urban films using a dynamic multimedia fugacity model. *Chemosphere*. 2012;87:1024-1031.
7. Wallace LA, Ott WR, Weschler CJ. Ultrafine particles from electric appliances and cooking pans: experiments suggesting desorption/nucleation of sorbed organics as the primary source. *Indoor Air*. 2015;25:536-546.
8. Wallace LA, Ott WR, Weschler CJ, Lai ACK. Desorption of SVOCs from heated surfaces in the form of ultrafine particles. *Environ Sci Technol*. 2017;51:1140-1146.
9. Bennett DH, Moran RE, Wu X, Tulse NS, Clifton MS, Colón M, et al. Polybrominated diphenyl ether (PBDE) concentrations and resulting exposure in homes in California: relationships among passive air, surface wipe and dust concentrations, and temporal variability. *Indoor Air*. 2015;25:220-229.
10. Bi CY, Liang YR, Xu Y. Fate and transport of phthalates in indoor environments and the influence of temperature: A case study in a test house. *Environ Sci Technol*. 2015;49:9674-9681.
11. Butt CM, Diamond ML, Truong J, Ikonomou MG, Ter Schure AFH. Spatial distribution of polybrominated diphenyl ethers in southern Ontario as measured in indoor and outdoor window organic films. *Environ Sci Technol*. 2004;38:724-731.
12. Cetin B, Odabasi M. Polybrominated diphenyl ethers (PBDEs) in indoor and outdoor window organic films in Izmir, Turkey. *J Hazard Mater*. 2011;185:784-791.
13. Duigu JR, Ayoko GA, Kokot S. The relationship between building characteristics and the



chemical composition of surface films found on glass windows in Brisbane, Australia. *Build Environ.* 2009;44:2228-2235.

14. Gao W, Wu J, Wang Y, Jiang G. Distribution and congener profiles of short-chain chlorinated paraffins in indoor/outdoor glass window surface films and their film-air partitioning in Beijing, China. *Chemosphere.* 2016;144:1327-1333.
15. Gewurtz SB, Bhavsar SP, Crozier PW, Diamond ML, Helm PA, Marvin CH, et al. Perfluoroalkyl contaminants in window film: Indoor/outdoor, urban/rural, and winter/summer contamination and assessment of carpet as a possible source. *Environ Sci Technol.* 2009;43:7317-7323.
16. Huo CY, Liu LY, Zhang ZF, Ma WL, Song WW, Li HL, et al. Phthalate esters in indoor window films in a northeastern Chinese urban center: Film growth and implications for human exposure. *Environ Sci Technol.* 2016;50:7743-7751.
17. Li J, Lin T, Pan SH, Xu Y, Liu X, Zhang C, et al. Carbonaceous matter and PBDEs on indoor/outdoor glass window surfaces in Guangzhou and Hong Kong, South China. *Atmos Environ.* 2010;44:3254-3260.
18. Melymuk L, Bohlin-Nizzetto P, Vojta S, Krátká M, Kukučka P, Audy O, et al. Distribution of legacy and emerging semivolatile organic compounds in five indoor matrices in a residential environment. *Chemosphere.* 2016;153:179-186.
19. Pan SH, Li J, Lin T, Zhang G, Li XD, Yin H, Polycyclic aromatic hydrocarbons on indoor/outdoor glass window surfaces in Guangzhou and Hong Kong, south China. *Environ Pollut.* 2012;169:190-195.
20. Venier M, Audy O, Vojta Š, Bečanová J, Romanak K, Melymuk L, et al. Brominated flame retardants in the indoor environment — Comparative study of indoor contamination from three countries. *Environ Int.* 2016;94:150-160.
21. Liu QT, Chen R, McCarry BE, Diamond ML, Bahavar B. Characterization of polar organic compounds in the organic film on indoor and outdoor glass windows. *Environ Sci Technol.* 2003;37:2340-2349.
22. Lam B, Diamond ML, Simpson AJ, Makar PA, Truong J, Hernandez-Martinez NA. Chemical composition of surface films on glass windows and implications for atmospheric chemistry. *Atmos Environ.* 2005;39:6578-6586.
23. Weschler CJ, Nazaroff WW. SVOC exposure indoors: fresh look at dermal pathways. *Indoor Air.* 2012;22:356-377.

24. Wu Y, Eichler CMA, Leng W, Cox SS, Marr LC, Little JC. Adsorption of phthalates on impervious indoor surfaces. *Environ Sci Technol*. 2017; doi: 10.1021/acs.est.6b05853.
25. Liang Y, Xu Y. The influence of surface sorption and air flow rate on phthalate emissions from vinyl flooring: Measurement and modeling. *Atmos Environ*. 2015;103:147-155.
26. Pedersen EK, Bjørseth O, Syversen T, Mathiesen M. A screening assessment of emissions of volatile organic compounds and particles from heated indoor dust samples. *Indoor Air*. 2003; 13:106-117.
27. Bhangar S, Mullen NA, Hering SV, Kreisberg NM, Nazaroff WW. Ultrafine particle concentrations and exposures in seven residences in northern California. *Indoor Air*. 2011;21:132-144.
28. Schripp T, Kirsch I, Salthammer T. Characterization of particle emission from household electrical appliances. *Sci Total Environ*. 2011;409:2534–2540.
29. Morgan MK, Sheldon LS, Croghan CW, Chuang JC, Lordo RA, Wilson NK, et al. A pilot study of children's total exposure to persistent pesticides and other persistent organic pollutants (CTEPP). EPA/600/R-041-193. Research Triangle Park, NC: US EPA National Exposure Research Laboratory: 2004.
30. Grøntoft T, Raychaudhuri MR. Compilation of tables of surface deposition velocities for O<sub>3</sub>, NO<sub>2</sub> and SO<sub>2</sub> to a range of indoor surfaces. *Atmos Environ*. 2004;38:533-544.
31. Klenø JG, Clausen PA, Weschler CJ, Wolkoff P. Determination of ozone removal rates by selected building products using the FLEC emission cell. *Environ Sci Technol*. 2001; 35:2548-2553.
32. Reiss R, Ryan PB, Koutrakis P. Modeling ozone deposition onto indoor residential surfaces. *Environ Sci Technol*. 1994;28:504-513.
33. Sabersky RH, Sinema DA, Shair FH. Concentrations, decay rates, and removal of ozone and their relation to establishing clean indoor air. *Environ Sci Technol*. 1973;7:347-353.
34. Lee K, Vallarino J, Dumyahn T, Özkaynak H, Spengler JD. Ozone decay rates in residences. *J Air Waste Manag Assoc*. 1999;49:1238-1244.
35. Nazaroff WW, Gadgil AJ, Weschler CJ. Critique of the use of deposition velocity in modeling indoor air quality. In Nagda NL, Ed., *Modeling of Indoor Air Quality and Exposure*, ASTM STP 1205, American Society for Testing and Materials, Philadelphia, 1993, pp. 81-104.
36. Weschler CJ. Ozone in indoor environments: Concentration and chemistry. *Indoor Air*.

2000;10:269-288.

37. Donahue NM, Robinson AL, Stanier CO, Pandis SN. Coupled partitioning, dilution, and chemical aging of semivolatile organics. *Environ Sci Technol*. 2006;40:2635-2643.
38. Weschler CJ, Nazaroff WW. SVOC partitioning between the gas phase and settled dust indoors. *Atmos Environ*. 2010;44:3609-3620.
39. Rudel RA, Camann DE, Spengler JD, Korn LR, Brody JG. Phthalates, alkylphenols, pesticides, polybrominated diphenyl ethers, and other endocrine-disrupting compounds in indoor air and dust. *Environ Sci Technol*. 2003;37:4543-4553.
40. Rudel RA, Dodson RE, Perovich LJ, Morello-Frosch R, Camann DE, Zuniga MM, et al. Semivolatile endocrine-disrupting compounds in paired indoor and outdoor air in two northern California communities. *Environ Sci Technol*. 2010;44:6583-6590.
41. Blanchard O, Glorennec P, Mercier F, Bonvallot N, Chevrier C, Ramalho O, et al. Semivolatile organic compounds in indoor air and settled dust in 30 French dwellings. *Environ Sci Technol*. 2014;48:3959-3969.
42. Liagkouridis I, Cousins AP, Cousins IT. Physical–chemical properties and evaluative fate modelling of ‘emerging’ and ‘novel’ brominated and organophosphorus flame retardants in the indoor and outdoor environment. *Sci Total Environ*. 2015;524–525:416-426.
43. Nicolaides N. Skin lipids: their biochemical uniqueness. *Science* 1974;186:19-26.
44. Xiao H, Wania F. Is vapor pressure or the octanol-air partition coefficient a better descriptor of the partitioning between gas phase and organic matter? *Atmos Environ*. 2003;37:2867-2878.
45. Cappa CD, Jimenez JL. Quantitative estimates of the volatility of ambient organic aerosol. *Atmos Chem Phys*. 2010;10:5409-5424.
46. Tang X, Misztal PK, Nazaroff WW, Goldstein AH. Volatile organic compound emissions from humans indoors. *Environ Sci Technol*. 2016;50:12686-12694.
47. Zhou S, Forbes MW, Abbatt JPD. Kinetics and products from heterogeneous oxidation of squalene with ozone. *Environ Sci Technol*. 2016;50:11688-11697.
48. Tolocka MP, Jang M, Ginter JM, Cox FJ, Kamens RM, Johnston MV. Formation of oligomers in secondary organic aerosol. *Environ Sci Technol*. 2004;38:1428-1434.
49. Koop T, Bookhold J, Shiraiwa M, Poschl U. Glass transition and phase state of organic compounds: dependency on molecular properties and implications for secondary organic aerosols in the atmosphere. *Phys Chemistry Chem Phys* 2011;13:19238-19255.

50. Gill PS, Graedel TE, Weschler CJ. Organic films on atmospheric aerosol particles, fog droplets, cloud droplets, raindrops, and snowflakes. *Rev Geophys.* 1983;21:903-920.
51. Donaldson DJ, Vaida V. The influence of organic films at the air-aqueous boundary on atmospheric processes. *Chem Rev.* 2006;106:1445-1461.
52. Krechmer JE, Pagonis D, Ziemann PJ, Jimenez JL. Quantification of gas-wall partitioning in Teflon environmental chambers using rapid bursts of low-volatility oxidized species generated in situ. *Environmental Science & Technology* 2016, 50:5757-5765.

**Figure 1.** Equilibrium sorptive partitioning of SVOCs in an organic film on an impermeable surface as a function of  $\log K_{oa}$ . Modeled conditions: film thickness = 10 nm; TSP =  $20 \mu\text{g m}^{-3}$ ;  $f_{om\_TSP} = 0.4$ ; and  $C_{ti} = 1 \mu\text{g m}^{-3}$  in each  $\log K_{oa}$  bin.

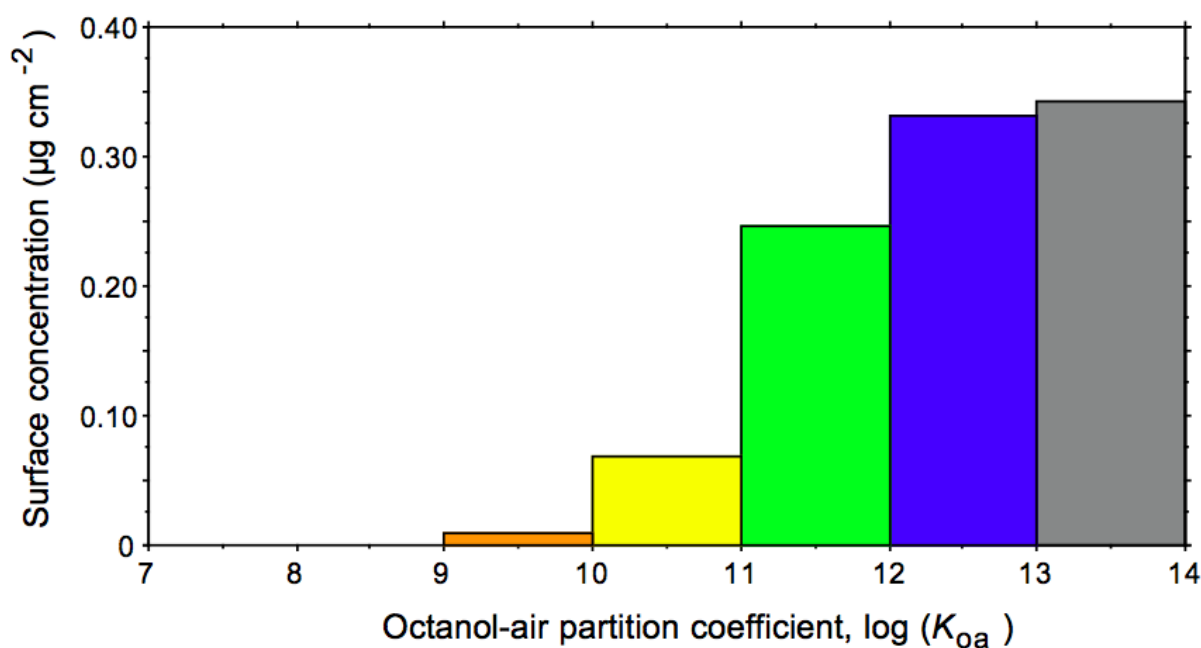


**Figure 2.** Evolution of organic surface film thickness predicted using a multicomponent partitioning model. In both cases, common assumptions are initial film thickness = 2 nm; TSP = 20  $\mu\text{g m}^{-3}$ ; and  $f_{\text{om-TSP}} = 0.4$ . For (a),  $C_{\text{ti}} = 4 \mu\text{g m}^{-3}$  in each of the five  $\log K_{\text{oa}}$  bins of unit width and centered at 8.5, 9.5, 10.5, 11.5 and 12.5. For (b),  $C_{\text{ti}} = 20, 15, 10, 5$  and  $2 \mu\text{g m}^{-3}$ , respectively, for the five same  $\log K_{\text{oa}}$  bins. Note that the bin for  $\log(K_{\text{oa}}) = 8-9$  contributes to film thickness imperceptibly in (a) and only slightly in (b).

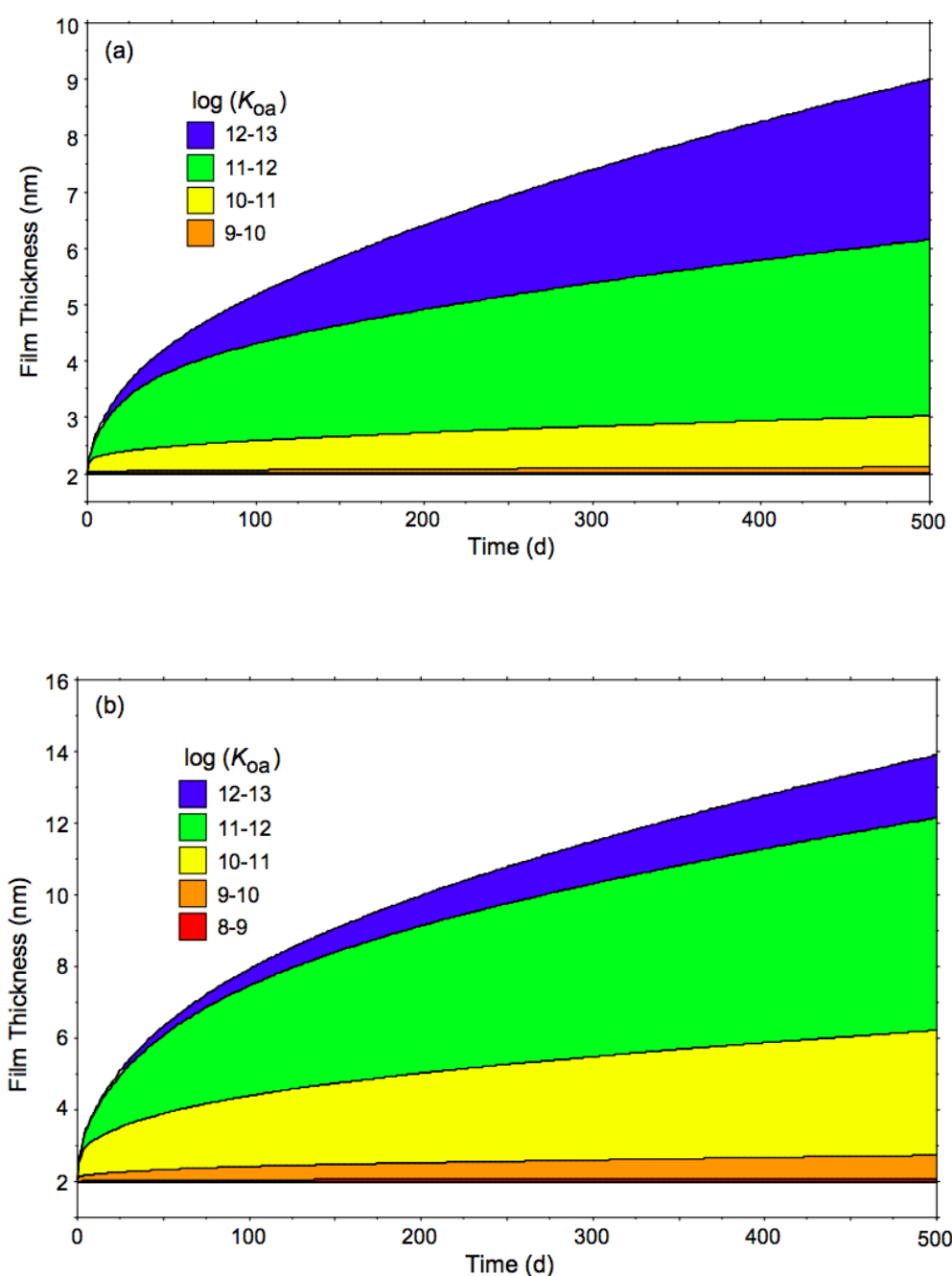


**Figure 3.** Modeled net absorption of BDE-47 and BDE-99 in an organic surface film as it evolves over a 500-day period on an initially clean, impermeable surface at 25 °C. The airborne concentrations,  $C_{ti}$ , of BDE-47 and BDE-99 match median values reported in Venier et al.<sup>20</sup> For these model calculations initial film thickness = 2 nm; TSP = 20  $\mu\text{g m}^{-3}$ ;  $f_{om\_TSP}$  = 0.4, and the total airborne concentrations of SVOC clusters are  $C_{ti}$  = 15, 10, 5 and 2  $\mu\text{g m}^{-3}$ , respectively, for log  $K_{oa}$  bins centered at 9.5, 10.5, 11.5 and 12.5.

